CERN-TH/97-30
ROME 97/1168
ROM2F /97/09

CHARMING PENGUINS IN B DECAYS

M. Ciuchini[1,⋆], E. Franco[2], G. Martinelli[2], L. Silvestrini[3]
[1] Theory Division, CERN, 1211 Geneva 23, Switzerland.
[2] Dip. di Fisica, Univ. "La Sapienza" and INFN,
Sezione di Roma, P.le A. Moro, I-00185 Rome, Italy.
[3] Dip. di Fisica, Univ. di Roma "Tor Vergata" and INFN,
Sezione di Roma II, Via della Ricerca Scientifica 1, I-00133 Rome, Italy.

Abstract

Full expressions of the $B^0_d \to \pi^+\pi^-$ and $B^0_d \to \pi^0\pi^0$ amplitudes, given in terms of matrix elements of operators of the effective weak Hamiltonian, are used to study the dependence of the relevant branching ratios on the different contributions. The uncertainty in the extraction of the weak phase α from the measurement of the time-dependent asymmetry in $B^0_d \to \pi^+\pi^-$ decays is also analyzed. We find that, among several effects which may enhance the $B^0_d \to \pi^0\pi^0$ branching ratio, the most important is due to "charming penguin" diagrams that have never been studied before. These diagrams easily increase $BR(B^0_d \to \pi^0\pi^0)$ up to a value of 1–3 $\times 10^{-6}$. The same effect produces, however, a large error in the extraction of α from the measurement of the $B^0_d \to \pi^+\pi^-$ time-dependent asymmetry. We show that it is possible to determine charming-penguin amplitudes from the experimental measurement of many decay rates. Their effect is impressive in $B^+ \to \pi^+K^0$ and $B^0_d \to K^+\pi^-$ decays, where charming-penguin contributions easily give values of $BR(B^+ \to \pi^+K^0)$ and $BR(B^0_d \to K^+\pi^-)$ of about 1×10^{-5}. Among other possibilities, we also suggest to use $B^0_d \to K^0\bar{K}^0$, the BR of which can be as large as 2–3 $\times 10^{-6}$, to determine the size of charming-penguin amplitudes.

⋆ On leave of absence from INFN, Sezione Sanità, V.le Regina Elena 299, Rome, Italy.

1 Introduction

The study of $B_d^0 \to \pi\pi$ ($\bar{B}_d^0 \to \pi\pi$) decays is of paramount importance for our understanding of CP-violation in the Standard Model and beyond. In particular the measurement of the time-dependent asymmetry

$$\begin{aligned} \mathcal{A}(t) &= \frac{N(B_d^0 \to \pi^+\pi^-)(t) - N(\bar{B}_d^0 \to \pi^+\pi^-)(t)}{N(B_d^0 \to \pi^+\pi^-)(t) + N(\bar{B}_d^0 \to \pi^+\pi^-)(t)} \\ &= \frac{(1-|\lambda|^2)\cos(\Delta M_d t) - 2Im\lambda \sin(\Delta M_d t)}{1+|\lambda|^2} \end{aligned} \tag{1}$$

may allow the extraction of the CP-violating phase α, see for example [1]. The cleanest method to extract $\sin 2\alpha$ is from the measurement of the asymmetry, combined with the separate determination of the $I = 0$ and $I = 2$ decay amplitudes, including the relative phase [2]. These can be obtained by measuring the $B^+ \to \pi^+\pi^0$, $B_d^0 \to \pi^+\pi^-$ and $B_d^0 \to \pi^0\pi^0$ (and the corresponding ones in the $\bar{B}_d^0$ case) branching ratios. With these measurements, we get rid of our ignorance of the hadronic matrix elements of the weak Hamiltonian. Unfortunately, most of the theoretical analyses tend to predict a very small $B_d^0 \to \pi^0\pi^0$ branching ratio, thus making the model-independent extraction of $\sin 2\alpha$ impossible in practice.

If $\sin 2\alpha$ has to be extracted from $B_d^0 \to \pi^+\pi^-$ only, the main uncertainty comes from the contribution proportional to $\lambda_t = V_{td}V_{tb}^\star$, which is usually called "penguin pollution". In several studies, the decay rates and the uncertainty of $\sin 2\alpha$ have been estimated by using some specific model to evaluate the hadronic matrix elements of the four-fermion operators entering the effective weak Hamiltonian [3]–[5]. In the most popular approaches the amplitudes have been computed by assuming the factorization hypothesis. The matrix elements of the weak currents necessary for the evaluation of the factorized amplitudes are then taken from a specific quark model or from the HQET [6]–[8].

In this paper, we present a "model-independent" analysis of the uncertainty on $\sin 2\alpha$ and of the ratio $R = \Gamma(B_d^0 \to \pi^0\pi^0)/\Gamma(B_d^0 \to \pi^+\pi^-)$. By "model-independent" we mean that we do not make specific assumptions on the hadronic matrix elements of the operators, such as factorization or the absence of final state interactions (FSI). On the basis of simple "qualitative" physical considerations, we allow, instead, the matrix elements to vary within certain "reasonable" ranges, and check the stability of the results against such variations. This is particularly relevant for R, because of the delicate cancellations occurring between different amplitudes present in the $B_d^0 \to \pi^0\pi^0$ case. Indeed, for this decay, the assumption of factorization and of the absence of FSI, or any approximation used to predict the value of the amplitude, may lead to an underestimate of the value of the decay rate.

Our calculations are based on complete expressions of the decays amplitudes for $B^+ \to \pi^+\pi^0$, $B_d^0 \to \pi^+\pi^-$ and $B_d^0 \to \pi^0\pi^0$, given in terms of diagrams representing Wick contractions of the operators of the effective Hamiltonian between the relevant external states. These formulae allow us to clarify assumptions and approximations usually made to evaluate the amplitudes, which have not been spelt explicitly in previous studies. In particular, we show the presence of diagrams, involving operators containing charmed quarks (defined as Q_1 and Q_2 in sec. 2) that contribute to the

penguin pollution, and that have never been considered before. We call these diagrams "charming penguins".

Among several effects which are able to enhance the $B_d^0 \to \pi^0\pi^0$ branching ratio, the most remarkable is due precisely to charming penguins. Their contribution may increase the estimate of $BR(B_d^0 \to \pi^0\pi^0)$ up to a value of 1–3 $\times 10^{-6}$. The reason is that, unlike the case of the penguin operators Q_3–Q_{10} which have small Wilson coefficients (of order $\alpha_s/12\pi \ln(m_t^2/\mu^2)$), the coefficients of Q_1 and Q_2 are of $O(1)$ and there is no reason to believe the corresponding matrix elements to be small. Charming penguins are also relevant for the $B_d^0 \to \pi^+\pi^-$ amplitude and may give a large shift $\Delta = \sin 2\alpha^{eff} - \sin 2\alpha \sim 0.4$–$0.8$ between the physical value of $\sin 2\alpha$ and the "effective" value, $\sin 2\alpha^{eff}$, which can be extracted from the experimental measurement of $Im\lambda$. As a comparison, when charming penguins are not included, the typical value is $\Delta \sim 0.1$. As Δ increases, however, also $BR(B_d^0 \to \pi^0\pi^0)$ becomes larger, thus opening the possibility of extracting $\sin 2\alpha$ with the isospin analysis proposed in ref. [2].

We finally show that many decay rates are expected to be dominated by charming-penguin diagrams. Among the various possibilities, we consider $B_d^0 \to K^0\bar{K}^0$, $B^+ \to \pi^+K^0$ and $B_d^0 \to K^+\pi^-$ decays. In these cases, we give explicit formulae for the amplitudes, show that the largest contributions are those expected from charming penguins and estimate the corresponding branching ratios.

The most impressive effect of charming penguins is found in $B^+ \to \pi^+K^0$ and $B_d^0 \to K^+\pi^-$ decays. Assuming reasonable values for the charming-penguin contributions, we find that their branching ratios may even become larger than $BR(B_d^0 \to \pi^+\pi^-)$. This observation is particularly interesting because, in absence of charming-penguin diagrams, the $B^+ \to \pi^+K^0$ and $B_d^0 \to K^+\pi^-$ rates turn out to be very small either because there is a Cabibbo suppression or because the non-Cabibbo suppressed terms come from penguin operators which have rather small Wilson coefficients (unless the corresponding matrix elements are exceedingly large). While finishing this analysis, we were informed that the CLEO collaboration has measured $BR(B_d^0 \to K^+\pi^-) = (1.5^{+0.5}_{-0.4} \pm 0.2) \times 10^{-5}$ [9]. The prediction that charming-penguin diagrams are important and give large $B^+ \to \pi^+K^0$ and $B_d^0 \to K^+\pi^-$ decay rates is supported by this measurement. By using the experimental information, we predict $BR(B^+ \to \pi^+K^0) \sim 1 \times 10^{-5}$ and we call for a search of this decay mode.

Other interesting decay channels, where charming penguins are expected to play an important role, such as $B_d^0 \to \pi^0\eta$ (or η'), $B_d^0 \to \phi K^0$ or $B_d^0 \to \eta\eta$ decays, will be extensively discussed elsewhere [10].

The plan of this paper is the following. In section 2, we introduce the effective Hamiltonian given in terms of four-fermion operators, and of the corresponding Wilson coefficients; we also define the full set of diagrams in terms of which the $B \to \pi\pi$ amplitudes can be expressed; the final formulae of the different amplitudes are given at the end of this section. Formulae and approximations for the $B_d^0 \to K^0\bar{K}^0$, $B^+ \to \pi^+K^0$ and $B_d^0 \to K^+\pi^-$ amplitudes are discussed in section 3. In section 4, we present several physical arguments which are used to guide us in estimating the matrix elements; we also explain the main criteria used in the numerical analysis. In section 5, we give and discuss the main numerical results for R, $\sin 2\alpha$ and for the $B_d^0 \to K^0\bar{K}^0$, $B^+ \to \pi^+K^0$ and $B_d^0 \to K^+\pi^-$ branching ratios.

2 Relevant formulae for $B \to \pi\pi$ decays

The effective weak Hamiltonian relevant for $B \to \pi\pi$ decays is given by

$$\begin{aligned}\mathcal{H}_{eff}^{\Delta B=1} &= \lambda_u \frac{G_F}{\sqrt{2}}\Big[\Big(C_1(\mu)\,(Q_1^u(\mu) - Q_1(\mu)) + C_2(\mu)\,(Q_2^u(\mu) - Q_2(\mu))\Big) \\ &+ \tau\,\vec{C}(\mu)\cdot\vec{Q}(\mu)\Big] \end{aligned} \tag{2}$$

where $\vec{Q}(\mu) = (Q_1(\mu), Q_2(\mu), \ldots, Q_{10}(\mu))$, $\vec{C}(\mu) = (C_1(\mu), C_2(\mu), \ldots, C_{10}(\mu))$, $\lambda_u = V_{ud}V_{ub}^\star$ and similarly λ_c and λ_t; $\tau = -\lambda_t/\lambda_u$ and μ is the renormalization scale of the operators Q_i. A convenient basis of operators [11]–[14], when QCD and QED corrections are taken into account, is

$$\begin{aligned} Q_1^u &= (\bar{b}d)_{(V-A)}(\bar{u}u)_{(V-A)} \\ Q_2^u &= (\bar{b}u)_{(V-A)}(\bar{u}d)_{(V-A)} \\ Q_1 &= (\bar{b}d)_{(V-A)}(\bar{c}c)_{(V-A)} \\ Q_2 &= (\bar{b}c)_{(V-A)}(\bar{c}d)_{(V-A)} \\ Q_{3,5} &= (\bar{b}d)_{(V-A)}\sum_q(\bar{q}q)_{(V\mp A)} \\ Q_4 &= \sum_q(\bar{b}q)_{(V-A)}(\bar{q}d)_{(V-A)} \\ Q_6 &= -2\sum_q(\bar{b}q)_{(S+P)}(\bar{q}d)_{(S-P)} \\ Q_{7,9} &= \frac{3}{2}(\bar{b}d)_{(V-A)}\sum_q e_q(\bar{q}q)_{(V\pm A)} \\ Q_8 &= -3\sum_q e_q(\bar{b}q)_{(S+P)}(\bar{q}d)_{(S-P)} \\ Q_{10} &= \frac{3}{2}\sum_q e_q(\bar{b}q)_{(V-A)}(\bar{q}d)_{(V-A)} \end{aligned} \tag{3}$$

where the subscripts $(V \pm A)$ and $(S \pm P)$ indicate the chiral structures and e_q denotes the quark electric charge ($e_u = 2/3$, $e_d = -1/3$, etc.). The sum over the quarks q runs over the active flavours at the scale μ.

Wick contractions of $\mathcal{H}_{eff}$ between hadronic states give rise to the diagrams shown in figs. 1–2: these are "Disconnected Emission" (DE), denoted also as T or T' in ref. [15]; the colour suppressed (non-factorizable) "Connected Emission" (CE), denoted also as C or C'; "Disconnected Annihilation" (DA), denoted also as A or A'; "Connected Annihilation" (CA), denoted also as E or E'; "Disconnected Penguin" (DP), "Connected Penguin" (CP), "Disconnected Penguin Annihilation" (DPA), "Connected Penguin Annihilation" (CPA). We assume $SU(2)$ isospin symmetry. For penguin diagrams, we introduce a label which identifies the quark flavour in the penguin loop. Thus, for example, $DP(s)$ denotes the disconnected penguin diagram DP of fig. 2, with a strange quark in the internal loop (a similar notation is adopted also for CP, DPA and CPA). Since we do not distinguish up and down quarks, we simply call DP (CP, DPA and CPA) those diagrams with an up or a down quark in the loop. In eq. (3), different Dirac structures appear, namely $L = (V-A)\times(V-A)$,

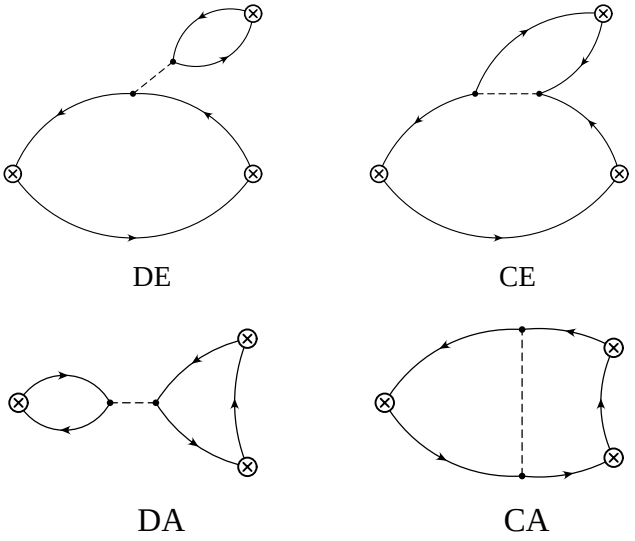

Figure 1: *Non-penguin diagrams. The dashed line represents the four-fermion operator.*

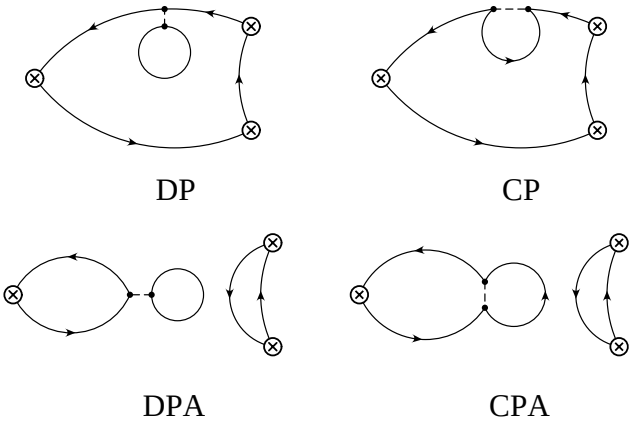

Figure 2: *Penguin diagrams.*

$R = (V-A)\times(V+A)$ and $S = (S+P)\times(S-P)$ [1]. Thus, for example, the notation CE_L and CE_S denote the connected emission diagrams with a $(V-A)\times(V-A)$ or $(S+P)\times(S-P)$ operator inserted, respectively. We are now ready to give the complete expressions for the decay amplitudes under study. It is convenient to write their $\Delta I = 3/2$ and $\Delta I = 1/2$ components separately

$$A^{+0} = A(B^+ \to \pi^+\pi^0) = \frac{G_F}{\sqrt{2}}\lambda_u \frac{3}{\sqrt{2}} A_2 \,, \tag{4}$$

$$A^{+-} = A(B_d^0 \to \pi^+\pi^-) = \frac{G_F}{\sqrt{2}}\lambda_u \left(A_2 - A_0\right) \,, \tag{5}$$

$$A^{00} = A(B_d^0 \to \pi^0\pi^0) = \frac{G_F}{\sqrt{2}}\lambda_u \left(\sqrt{2}A_2 + \frac{1}{\sqrt{2}} A_0\right) \,, \tag{6}$$

where

$$A_2 = A_2^u + \tau A_2^t \,, \qquad A_0 = A_0^u + \tau A_0^t \,, \tag{7}$$

and

$$A_2^u = -\frac{1}{3}\left[C_1 + C_2\right]\left(DE_L + CE_L\right) \tag{8}$$

$$\begin{aligned} A_2^t = & -\frac{1}{2}\left[C_7\left(DE_R + CE_R\right) - 2C_8\left(DE_S + CE_S\right)\right. \\ & \left. + \left(C_9 + C_{10}\right)\left(DE_L + CE_L\right)\right] \,, \end{aligned} \tag{9}$$

$$\begin{aligned} A_0^u = & \; C_1\left[-\frac{1}{3}DE_L + \frac{2}{3}CE_L + DA_L + \left(DP_L - DP_L(c)\right) + \left(DPA_L - DPA_L(c)\right)\right] \\ + & \; C_2\left[\frac{2}{3}DE_L - \frac{1}{3}CE_L + CA_L + \left(CP_L - CP_L(c)\right) + \left(CPA_L - CPA_L(c)\right)\right] \end{aligned} \tag{10}$$

$$\begin{aligned} A_0^t = & \; C_1\left[DP_L(c) + DPA_L(c)\right] + C_2\left[CP_L(c) + CPA_L(c)\right] \\ + & \; C_3\left[CE_L + CA_L + 2DA_L + CP_L + 2DP_L + DP_L(c) + DP_L(s)\right. \\ + & \; \left. CPA_L + 2DPA_L + DPA_L(c) + DPA_L(s)\right] \\ + & \; C_4\left[DE_L + 2CA_L + DA_L + 2CP_L + CP_L(c) + CP_L(s) + DP_L\right. \\ + & \; \left. 2CPA_L + CPA_L(c) + CPA_L(s) + DPA_L\right] \\ + & \; C_5\left[CE_R + CA_R + 2DA_R + CP_R + 2DP_R + DP_R(c) + DP_R(s)\right. \\ + & \; \left. CPA_R + 2DPA_R + DPA_R(c) + DPA_R(s)\right] \\ - & \; 2C_6\left[DE_S + 2CA_S + DA_S + 2CP_S + CP_S(c) + CP_S(s) + DP_S\right. \\ + & \; \left. 2CPA_S + CPA_S(c) + CPA_S(s) + DPA_S\right] \\ + & \; \frac{1}{2}C_7\left[CE_R - DE_R - CA_R + DA_R - CP_R + DP_R + 2DP_R(c) - DP_R(s)\right. \\ - & \; \left. CPA_R + DPA_R + 2DPA_R(c) - DPA_R(s)\right] \\ + & \; C_8\left[CE_S - DE_S - CA_S + DA_S - CP_S - 2CP_S(c) + CP_S(s) + DP_S\right. \\ - & \; \left. CPA_S - 2CPA_S(c) + CPA_S(s) + DPA_S\right] \end{aligned} \tag{11}$$

[1] By Fierz rearrangement we could have adopted a basis where only $(V-A)\times(V\pm A)$ structures are present. We prefer however to work with operators written in terms of colour-singlet bilinears.

$$
\begin{aligned}
+ \quad & \frac{1}{2} C_9 \left[CE_L - DE_L - CA_L + DA_L - CP_L + DP_L + 2DP_L(c) - DP_L(s) \right. \\
- \quad & \left. CPA_L + DPA_L + 2DPA_L(c) - DPA_L(s) \right] \\
- \quad & \frac{1}{2} C_{10} \left[CE_L - DE_L - CA_L + DA_L - CP_L - 2CP_L(c) + CP_L(s) + DP_L \right. \\
- \quad & \left. CPA_L - 2CPA_L(c) + CPA_L(s) + DPA_L \right] \ .
\end{aligned}
$$

In eqs. (8)–(11) we have not shown explicitly the argument μ of the Wilson coefficients $C_1, \ldots, C_{10}$. Notice that also the diagrams are μ-dependent, since they correspond to contractions of renormalized operators $Q_i(\mu)$. For the fields we have assumed the standard convention $B^+ = \bar{b}u$, $B_d^0 = \bar{b}d$, $\pi^+ = u\bar{d}$, $\pi^- = -d\bar{u}$ and $\pi^0 = -1/\sqrt{2}(u\bar{u} - d\bar{d})$.

In A_0^u, penguin diagrams always appear in the GIM combinations $DP_L - DP_L(c)$, $DPA_L - DPA_L(c)$, ... (in the following we denote these combinations as GIM-penguins). Had we taken $m_t \ll M_W$ and a renormalization scale μ larger than the top quark mass, i.e. $m_t \ll \mu \ll M_W$, similar GIM combinations would have appeared in A_0^t, namely $DP_L(t) - DP_L(c)$, etc. Since the physical value of m_t is so large, the diagrams $DP_L(t)$, $CP_L(t)$, etc. are replaced by complicated structures. These arise from the contractions of the penguin and electro-penguin operators Q_3–Q_{10}, originated in $\mathcal{H}_{eff}$ when we remove the top quark from the effective theory. In the literature, A_0^t only is identified as penguin pollution. We want to stress again that in the effective theory there are "penguin operators" Q_3–Q_{10}, which originate from the imperfect GIM cancellation occurring when $\mu \ll m_t$ and "penguin diagrams" which arise from the Wick contractions of *all* the operators of $\mathcal{H}_{eff}$.

The coefficients of the penguin operators Q_3–Q_{10} are of order $\alpha_s/12\pi \ln(m_t^2/\mu^2)$ and contain the short distance contribution (from scales between μ and m_t) of the virtual top and charm quarks. For $\mu \sim m_b$, these coefficients are rather small, e.g. the dominant term is due to Q_6, for which $C_6/C_2 \sim -0.03$. Thus, unless the corresponding matrix elements are very large, the penguin operators are not expected to give large corrections, at least in the $B_d^0 \to \pi^+\pi^-$ case. In the $B_d^0 \to \pi^0\pi^0$ case, the relative correction due to penguin operators, Q_6 in particular, may be more important due to the large cancellations present in the amplitude (the so called "colour suppression" to be discussed below).

This is not the end of the story, however. In A_0^t there are other terms, specifically those in the first line of eq. (11). These terms, denoted as "charming penguins", come from penguin contractions of the operators Q_1 and Q_2, and have to be understood as long distance contributions in the matrix elements of these operators. Because of the unitarity relation $\lambda_c = -\lambda_u - \lambda_t$, they give contributions to both A_0^u, in the GIM combination DP_L-$DP_L(c)$, and to A_0^t. Unlike the case of the penguin operators Q_3–Q_{10}, the coefficients of Q_1 and Q_2 are of $O(1)$ and, since there is no reason to believe the corresponding matrix elements to be small [2], they are potentially relevant even for the $B_d^0 \to \pi^+\pi^-$ amplitude. On the other hand We notice that their contribution can be further enhanced by the factor $|\tau| \sim 2$.

Penguin diagrams are also present in A_0^u and can alter in A^{+-} and A^{00} the relative size of the term proportional to λ_u with respect to that proportional to λ_t. This can

[2] This is true in spite of the fact that, for $(V-A) \times (V-A)$ operators, penguin diagrams vanish if we assume factorization, as demonstrated by the important role that they are expected to play in kaon decays.

be seen by looking to the expression of λ introduced in eq. (1) in terms of the different amplitudes

$$\lambda = \frac{q}{p}\frac{\overline{A}^{+-}}{A^{+-}} = \frac{q}{p}\frac{\lambda_u^\star}{\lambda_u}\frac{1+\tau^\star(A_2^t-A_0^t)/(A_2^u-A_0^u)}{1+\tau(A_2^t-A_0^t)/(A_2^u-A_0^u)}\ , \tag{12}$$

where

$$\begin{aligned}
\frac{q}{p} &= \frac{V_{td}V_{tb}^\star}{V_{td}^\star V_{tb}} = \frac{1-\rho-i\eta}{1-\rho+i\eta} = e^{-2i\beta} \\
\frac{\lambda_u^\star}{\lambda_u} &= \frac{V_{ub}V_{ud}^\star}{V_{ud}V_{ub}^\star} = \frac{\rho-i\eta}{\rho+i\eta} = e^{-2i\gamma} \\
\tau &= -\frac{1-\rho-i\eta}{\rho+i\eta}
\end{aligned} \tag{13}$$

ρ and η being the CKM parameters in the Wolfenstein parametrization [16] and $\beta+\gamma = \pi-\alpha$.

At this point we have all the formulae needed for the study of the uncertainties on $\sin 2\alpha$ and in the calculation of R.

3 $B_d^0 \to K^0\bar{K}^0$, $B^+ \to \pi^+K^0$ and $B_d^0 \to K^+\pi^-$

We now show that the $B_d^0 \to K^0\bar{K}^0$, $B^+ \to \pi^+K^0$ and $B_d^0 \to K^+\pi^-$ amplitudes are dominated by GIM- and charming-penguin diagrams. Let us consider the three cases separately. For simplicity, all the formulae in this section are computed in the $SU(3)$ symmetric limit, e.g. $DP_L(s) = DP_L$.

$\underline{B_d^0 \to K^0\bar{K}^0}$ We start by studying this case for which all the relevant quantities have already been defined. The amplitude is dominated by GIM and charming-penguin diagrams because emission and annihilation diagrams are only produced by the insertion of the operators Q_3–Q_{10} which have very small Wilson coefficients. By defining $A(B_d^0 \to K^0\bar{K}^0) = \lambda_u G_F/\sqrt{2} \times A_K$, the complete expression of A_K is given by

$$\begin{aligned}
A_K &= C_1\left[(DP_L - DP_L(c)) + \tau DP_L(c) + (DPA - DPA_L(c)) + \tau DPA_L(c)\right] \\
&+ C_2\left[(CP_L - CP_L(c)) + \tau CP_L(c) + (CPA - CPA_L(c)) + \tau CPA_L(c)\right] \\
&+ \tau\{C_3\left[CE_L + CA_L + 2DA_L + CP_L + 3DP_L + DP_L(c)\right. \\
&+ \left. CPA_L + 3DPA_L + DPA_L(c)\right] \\
&+ C_4\left[DE_L + 2CA_L + DA_L + 3CP_L + CP_L(c) + DP_L\right. \\
&+ \left. 3CPA_L + CPA_L(c) + DPA_L\right] \\
&+ C_5\left[CE_R + CA_R + 2DA_R + CP_R + 3DP_R + DP_R(c)\right. \\
&+ \left. CPA_R + 3DPA_R + DPA_R(c)\right] \\
&- 2C_6\left[DE_S + 2CA_S + DA_S + 3CP_S + CP_S(c) + DP_S\right. \\
&+ \left. 3CPA_S + CPA_S(c) + DPA_S\right] \\
&+ \frac{1}{2}C_7\left[-CE_R - CA_R - 2DA_R - CP_R + 2DP_R(c)\right. \\
&- \left. CPA_R + 2DPA_R(c)\right] \\
&+ C_8\left[DE_S + 2CA_S + DA_S - 2CP_S(c) + DP_S\right.
\end{aligned} \tag{14}$$

$$
\begin{aligned}
&- \quad 2CPA_S(c) + DPA_S] \\
&+ \quad \frac{1}{2}C_9\,[-CE_L - CA_L - 2DA_L - CP_L + 2DP_L(c) \\
&- \quad CPA_L + 2DPA_L(c)] \\
&- \quad \frac{1}{2}C_{10}\,[DE_L + 2CA_L + DA_L - 2CP_L(c) + DP_L \\
&- \quad 2CPA_L(c) + DPA_L]\} \ .
\end{aligned}
$$

By neglecting all penguin-operator contributions we get

$$
\begin{aligned}
A_K &= C_1\,[(DP_L - DP_L(c)) + \tau DP_L(c) + (DPA - DPA_L(c)) + \tau DPA_L(c)] \\
&+ C_2\,[(CP_L - CP_L(c)) + \tau CP_L(c) + (CPA - CPA_L(c)) + \tau CPA_L(c)] \ . \qquad (15)
\end{aligned}
$$

This shows that unless the matrix elements of penguin operators, Q_6 for example, are exceedingly large (much larger than their estimates in the factorization hypothesis [5]), the amplitude is dominated by GIM- and charming-penguin diagrams. Equation (15) is only given to display the relevant terms; in all our numerical calculations we always used the complete expressions for all the amplitudes.

$\underline{B^+ \to \pi^+ K^0}$ In order to study $B^+ \to \pi^+ K^0$ and $B_d^0 \to K^+\pi^-$ we have to introduce new quantities. For these decays, the operator Q_1^u is replaced by $Q_1'^u = (\bar{b}s)_{(V-A)}(\bar{u}u)_{(V-A)}$ with a Wilson coefficient $C_1' = C_1$, and similarly for all the other operators in (3): this comes from the fact that we are considering now $\Delta B = -\Delta S = 1$ transitions instead of the $\Delta B = \Delta D = 1$ ones of sec. 2. We also define $\lambda_u' = V_{us}V_{ub}^\star$ and similarly λ_c' and λ_t': λ_u' is of $O(\lambda^4)$ whereas λ_c' and λ_u' are of $O(\lambda^2)$, where $\lambda \sim 0.22$ is the sine of the Cabibbo angle in the Wolfenstein approximation. With the exception of $\lambda_{u,c,t}'$, we will omit the superscript $'$ for the rest of this section. We write

$$
A(B^+ \to \pi^+ K^0) = \frac{G_F}{\sqrt{2}}\Big(\lambda_u' A_+^u + \lambda_c' A_+^c + \lambda_t' A_+^t\Big)\,, \qquad (16)
$$

where

$$
\begin{aligned}
A_+^u &= C_1\,[CA_L + DP_L] + C_2\,[DA_L + CP_L] \\
A_+^c &= C_1 DP_L(c) + C_2 CP_L(c)
\end{aligned}
$$

$$
\begin{aligned}
A_+^t &= -C_3\,[CE_L + CA_L + CP_L + 3DP_L + DP_L(c)] \\
&- C_4\,[DE_L + DA_L + 3CP_L + CP_L(c) + DP_L] \\
&- C_5\,[CE_R + +CA_R + CP_R + 3DP_R + DP_R(c)] \\
&+ 2C_6\,[DE_S + DA_S + 3CP_S + CP_S(c) + +DP_S] \qquad (17) \\
&- \frac{1}{2}C_7\,[-CE_R + 2CA_R - CP_R + 2DP_R(c)] \\
&- C_8\,[DE_S - 2DA_S - 2CP_S(c) + DP_S] \\
&- \frac{1}{2}C_9\,[-CE_L + 2CA_L - CP_L + 2DP_L(c)] \\
&- \frac{1}{2}C_{10}\,[-DE_L + 2DA_L + 2CP_L(c) - DP_L] \ .
\end{aligned}
$$

By neglecting all penguin-operator contributions and Cabibbo suppressed terms we get

$$A(B^+ \to \pi^+ K^0) = \frac{G_F}{\sqrt{2}} \lambda'_c A^c_+ = \frac{G_F}{\sqrt{2}} \lambda'_c \left[C_1 DP_L(c) + C_2 CP_L(c) \right] , \tag{18}$$

$\underline{B^0_d \to K^+ \pi^-}$ We write

$$A(B^0_d \to K^+ \pi^) = \frac{G_F}{\sqrt{2}} \Big(\lambda'_u A^u_0 + \lambda'_c A^c_0 + \lambda'_t A^t_0 \Big) , \tag{19}$$

where

$$\begin{aligned} A^u_0 &= C_1 \left[-CE_L - DP_L \right] + C_2 \left[-DE_L - CP_L \right] \\ A^c_0 &= -C_1 DP_L(c) - C_2 CP_L(c) \end{aligned}$$

$$\begin{aligned} A^t_0 &= -C_3 \left[-CE_L - CA_L - CP_L - 3DP_L - DP_L(c) \right] \\ &- C_4 \left[-DE_L - DA_L - 3CP_L - CP_L(c) - DP_L \right] \\ &- C_5 \left[-CE_R - CA_R - CP_R - 3DP_R - DP_R(c) \right] \\ &+ 2C_6 \left[-DE_S - DA_S - 3CP_S - CP_S(c) - DP_S \right] \\ &- \frac{1}{2} C_7 \left[-2CE_R + CA_R + CP_R - 2DP_R(c) \right] \\ &- C_8 \left[2DE_S - DA_S + 2CP_S(c) - DP_S \right] \\ &- \frac{1}{2} C_9 \left[-2CE_L + CA_L + CP_L - 2DP_L(c) \right] \\ &- \frac{1}{2} C_{10} \left[-2DE_L + DA_L - 2CP_L(c) + DP_L \right] . \end{aligned} \tag{20}$$

By neglecting all penguin-operator contributions and Cabibbo suppressed terms we get

$$A(B^0_d \to K^+ \pi^-) = \frac{G_F}{\sqrt{2}} \lambda'_c A^c_0 = -\frac{G_F}{\sqrt{2}} \lambda'_c \left[C_1 DP_L(c) + C_2 CP_L(c) \right] , \tag{21}$$

In $A(B^+ \to \pi^+ K^0)$ and $A(B^0_d \to K^+ \pi^-)$, if charming-penguin diagrams are very small then both Cabibbo suppressed contributions and terms due to penguin operators must be included in the calculation since they are of the same size.

4 Estimates of the diagrams

In this section, we discuss the criteria adopted to evaluate the diagrams appearing in eqs. (8)-(11) and in sec. 3. Notice that the value of the diagrams is given only once that the renormalization prescription (RP) and renormalization scale μ of the operators have been fixed. Under a change of RP or μ the values of the diagrams must be changed in such a way as to compensate the corresponding changes of the Wilson coefficients C_i, thus giving the same physical predictions up to and including next-to-leading logarithmic corrections [17]–[22] [3]. The state of the art in the calculation of the

[3] Notice that under a change of the RP or of μ, contributions attributed to matrix elements of some operators can go into the Wilson coefficients or the matrix elements of others, and viceversa.

matrix elements of the operators is such that, given the complexity of the expressions in eqs. (8)–(11), this turns out to be impossible. For example, factorized amplitudes are RP and scale independent, being expressed in terms of physical quantities. Thus they cannot compensate a variation of the coefficient functions. On the other hand, the possibility that lattice calculations be able to compute (8)–(11) with sufficient accuracy appears to be rather remote. This is particularly true for A^{00} where delicate cancellations are likely to occur between different contributions, see also the discussion and the end of this section and section 5. In the following, in order to check the stability of the results, at fixed values of the diagrams we vary the Wilson coefficients by changing RP and by taking 2 GeV $\leq \mu \leq$ 10 GeV.

We now discuss the assumptions made in the evaluations of the different diagrams:

1) $\underline{DPA \text{ and } CPA}$ These are Zweig suppressed diagrams which we assume to give a negligible contribution.

2) Electro-penguins In order to monitor the effects of the electro-penguins, we only consider the contributions coming from the operators Q_9 and Q_{10} since these operators have coefficients much larger than Q_7 and Q_8.

3) $\underline{DE_L \text{ and } CE_L}$ In most of the theoretical analyses, these diagrams give the largest contribution to the $B_d^0 \to \pi\pi$ amplitudes. If only emissions are present, there are three independent quantities namely $|DE_L|$, $|CE_L|$ and $arg(DE_L \times CE_L^\star)$. Without loss of generality we can then write $CE_L = \xi DE_L e^{i\delta_\xi}$. We vary $0.0 \leq \xi \leq 0.5$: this range covers the value preferred by the analysis of D-meson two-body non-leptonic decays, which suggests $\xi \sim 0$, and the value derived from a_2/a_1 extracted from $B \to D\pi$ and $B \to D\rho$ decays [3, 23]. Moreover it includes the canonical value $\xi = 1/N_c$ where N_c is the number of colours. On the basis of some estimates of FSI [24, 25], we do not expect the relative phase δ_ξ to be larger than ~ 0.5, at the energy scales flowing into the pion system in B-decays. We enlarged the range of δ_ξ up to ~ 1 in order to check which kind of effect could be produced by a large phase.

4) $\underline{DA_L \text{ and } CA_L}$ These are diagrams usually neglected since arguments can be made that, in the factorization hypothesis, they are suppressed by a factor f_B/M_B (besides colour suppression in CA_L) [15]. f_B/M_B is related to the B-meson wave function in the origin. A further suppression factor comes from the matrix element of the divergence of the vector current which creates the pion pair. In ref. [26], however, a fit to two-body D-meson decays, resulted in a non negligible value for the annihilation diagrams, corresponding to $DA_L/DE_L \sim 0.3(m_s - m_d)/f_\pi$. It is not clear how these results should be scaled to the B-meson case and for degenerate quark masses.

   Rescattering effects, which have been shown to persist even for large quark masses [24], can also enhance the value of annihilation diagrams with respect to factorization estimates [27], see also [28]. As discussed in ref. [27], emission and annihilation diagrams are connected via FSI. For example, the CA-diagram can be seen as a DE followed by rescattering of the final states. In the $1/N_c$ expansion, since the scattering amplitude is of order $1/N_c$, this gives immediately the correct leading dependence on the number of colours for CA_L. In fact $DE_L \sim N_c^{1/2}$, $CA_L \sim N_c^{-1/2}$ and $CA_L \sim \eta_A DE_L$, where η_A is proportional to the scattering

amplitude, which is of $O(1/N_c)$. The only potentially large contribution from annihilation diagrams comes indeed from the term $\propto C_2\, CA_L$ in eq. (26), since all the other annihilation contributions (either DA_L or CA_L) have (much) smaller coefficients. Moreover, several arguments can be made to show that the value of DA_L is expected to be at most of the size of CA_L and its largest contribution multiplies C_1 which is about 1/5 of C_2. In our numerical analysis, we have explicitly checked, by varying DA_L between zero and CA_L, that its effect is rather marginal. For this reason, in sec. 5 we only discuss the case with $DA_L = 0$. To take into account rescattering effects, we parametrize CA_L as $CA_L = iDE_L\eta_A$. η_A is a complex "inelasticity" coefficient, the absolute value of which has been estimated to be of the order of some tenth [24, 25]. In our numerical study we take it real with $0 \leq \eta_A \leq 0.5$ [4]. The same rescattering mechanism relates disconnected and connected diagrams in the penguin case, which is discussed below.

5) GIM-penguins Penguin-like contractions appear both in A_0^u and A_0^t. Here following we discuss the two cases separately. In A_0^u we always find the combinations $DP_L - DP_L(c)$ and $CP_L - CP_L(c)$ and one could argue that, because of the large final state energy at disposal, GIM cancellation makes these contributions negligible. The GIM mechanism, however, is expected to be effective only at short distances, i.e. when a high momentum flows in the penguin loop. For low momenta, i.e. if we look to long-distance effects, these diagrams can also be interpreted as emission diagrams followed by rescattering. For example,

$$\begin{aligned} CP_L - CP_L(c) &\sim DE_L(B_d^0 \to \pi\pi) S_0(\pi\pi \to \pi\pi) \\ &\quad - DE_L(B_d^0 \to D\,D) S_0(D\,D \to \pi\pi) \\ &\sim f_\pi q^\mu \langle \pi(\vec{p}_B - \vec{q}) | J_\mu^{ub} | B_d^0 \rangle S_0(\pi\pi \to \pi\pi) \\ &\quad - f_D q^\mu \langle D(\vec{p}_B - \vec{q}) | J_\mu^{cb} | B_d^0 \rangle S_0(D\,D \to \pi\pi)\,, \end{aligned} \tag{22}$$

where S_0 is the strong interaction S-matrix and $J_\mu^{ub,cb}$ are the weak vector currents. Since $f_D/f_\pi \sim 1.5$ [29] and the form factors relative to $\langle \pi(\vec{p}_B - \vec{q}) | J_\mu^{bu} | B_d^0 \rangle$ are expected to be smaller than those relative to $\langle D(\vec{p}_B - \vec{q}) | J_\mu^{bc} | B_d^0 \rangle$ [6]–[8], by about a factor of 2, $F^{cb}(M_D^2) \sim 2\, F^{ub}(M_\pi^2)$, it is not clear how effective is the GIM cancellation between the two contributions. A large cancellation between the charm and up contributions may still take place if the relative factor $S_0(D\,D \to \pi\pi)/S_0(\pi\pi \to \pi\pi)$ compensates the differences due to phase space, decay constants and form factors [5].

The discussion of rescattering effects for GIM-penguins strictly follows that of the annihilation diagrams made in 4). For this reason, given our ignorance of S_0, we use the parametrization $CP_L - CP_L(c) = iDE_L\eta_P$, with $0 \leq \eta_P \leq 0.5$, and ignore the contribution from $DP_L - DP_L(c)$.

6) Other penguin diagrams In A_0^t, penguin contributions are not GIM suppressed. Thus we expect that rescattering effects play a minor role. Penguin contributions are of two kinds: either they correspond to the insertion of left-left operators, Q_1,

[4] All estimates give $Re\,\eta_A \gg Im\,\eta_A$ [24, 25].

[5] In this respect a combined measurement of the $B \to \pi\pi$ and $B \to D\,D$ branching ratios would be very interesting.

Q_2, Q_3, Q_4, Q_9 and Q_{10}, or they are given by the insertion of Q_5 and Q_6, for example in DP_R or DP_S.

In the previous section, we have noticed that penguin contractions of the operators Q_1 and Q_2 can give large effects since the corresponding coefficients are of $O(1)$. In our numerical analysis we find that a modest relative phase between DP_L and CP_L can have dramatic effects. For this reason we introduce two parameters η_L and δ_L, by writing $DP_L = |DE_L|\eta_L$ and $CP_L = e^{i\delta_L}|CE_L|\eta_L$, with $0.0 \leq \eta_L \leq 1.2$ and $0 \leq \delta_L \leq 0.5$. The range of values of η_L is dictated from the fact that there is no reason to expect very large/small values for these matrix elements, so we take them of the same order than the corresponding emission diagrams. As for the phase, we limit the maximum of δ_L to 0.5, as we did for δ_ξ. For simplicity, we take η_L flavour independent, i.e. we use the same value of η_L for DP_L, $DP_L(s)$ and $DP_L(c)$. We do not connect CP_L to DE_L, as we did for GIM-penguins, because, as said above, we do not have to advocate long-distance effects coming from emissions followed by rescattering. In general, we should consider a complex value of η_L. We checked, however, that the largest effects come from the relative phase between DP_L and CP_L and for this reason, only the case with η_L real will be discussed in the following.

Left-right penguin contributions only appear together with all the other contractions of Q_5 and Q_6. The latter have the same topology of the diagrams considered so far, but different chiral structures. Rather than introducing another set of free parameters for the $(V-A)\times(V+A)$ and $(S+P)\times(S-P)$ diagrams, we consider globally the matrix elements of the operators Q_5 and Q_6 and write

$$\langle\pi\pi|Q_5|B_d^0\rangle = \eta_5 CE_L\,, \qquad \langle\pi\pi|Q_6|B_d^0\rangle = \eta_6 DE_L\,. \tag{23}$$

In kaon decays, there is a common prejudice that the operators Q_5 and Q_6 trigger the octet enhancement [6]. If really the explanation of the enhancement relies on the matrix elements of these operators (as also suggested by lattice calculations [30]), then $\eta_{5,6}$ can be as large as 5. Since the kinematical configuration is so different in B-decays, due to the large mass of the b-quark, and many of the arguments for the enhancement are based on the chiral expansion, we do not really expect $\eta_{5,6}$ to be as large as in the kaon case. Since we cannot exclude, however, values of $O(1)$, we vary $0.0 \leq \eta_{5,6} \leq 2.0$.

We summarize the discussion above, by giving the expressions (8)–(11) in units of DE_L, and in terms of the parameters ξ, δ_ξ, δ_L and of the η_is

$$A_2^u = -\frac{1}{3}\left(C_1 + C_2\right)\left(1 + \xi e^{i\delta_\xi}\right) \tag{24}$$

$$A_2^t = -\frac{1}{2}\left(C_9 + C_{10}\right)\left(1 + \xi e^{i\delta_\xi}\right)\,, \tag{25}$$

$$A_0^u = C_1\left[-\frac{1}{3} + \frac{2}{3}\xi e^{i\delta_\xi}\right]$$

[6] In the kaon case, if μ is larger than the charm mass, which plays the role of the top quark mass for GIM effects, the operators Q_5 and Q_6 are hidden in the matrix elements of $Q_1^u - Q_1$ and $Q_2^u - Q_2$ (with $b \to s$ in the operators of the effective Hamiltonian) .

$$
\begin{aligned}
&+ \quad C_2\left[\frac{2}{3}-\frac{1}{3}\xi e^{i\delta_\xi}+i(\eta_A+\eta_P)\right] && (26)\\
A_0^t &= \left[C_1+C_2\xi e^{i\delta_L}\right]\eta_L + \\
&+ \quad C_3\left[\xi e^{i\delta_\xi}+i\eta_A+\left(4+\xi e^{i\delta_L}\right)\eta_L\right] \\
&+ \quad C_4\left[1+2i\eta_A+(1+4\xi e^{i\delta_L})\eta_L\right] \\
&+ \quad C_5\xi e^{i\delta_\xi}\eta_5+C_6\eta_6 \\
&+ \quad \frac{1}{2}C_9\left[-1+\xi e^{i\delta_\xi}-i\eta_A+\left(2-\xi e^{i\delta_L}\right)\eta_L\right] \\
&- \quad \frac{1}{2}C_{10}\left[-1+\xi e^{i\delta_\xi}-i\eta_A+\left(1-2\xi e^{i\delta_L}\right)\eta_L\right]\,. && (27)
\end{aligned}
$$

Before discussing the numerical results of our analysis, we want to add some observations about colour-suppressed processes. The starting point are eqs. (8)–(11) [(24)–(27)], which contain the expressions of the relevant amplitudes. For the sake of illustration, let us consider first the case where only DE_L and CE_L are non vanishing and we neglect penguin operator contributions. In this case, when we insert (8)–(11) in eqs. (5) and (6) the following combinations occur

$$
\begin{aligned}
A^{+-} &\propto C_1CE_L+C_2DE_L = C_2DE_L\left(1+\frac{C_1}{C_2}\xi e^{i\delta_\xi}\right) && (28)\\
A^{00} &\propto C_1DE_L+C_2CE_L = C_1DE_L\left(1+\frac{C_2}{C_1}\xi e^{i\delta_\xi}\right)\,. && (29)
\end{aligned}
$$

Numerically, the ratio $-C_1/C_2\sim 0.2$–0.3 is approximatively equal in size and opposite in sign to the expected value of ξ. This implies that the second term in eq. (28) is a small correction (of the order of 10%) to the first one while the two terms in eq. (29) tend to cancel (for small values of the phase δ_ξ). This, together with the smallness of C_1, is at the origin of colour suppression. In D-decays, where a very small value of ξ is preferred, colour suppression is expected to be less effective [7].

As can be read from eqs. (8)–(11), a similar colour-suppression pattern is present in all the $\Delta I=1/2$ annihilation and penguin diagrams generated by the operators Q_1–Q_2, which are the operators with the largest coefficients:

$$
\begin{aligned}
A^{00} &\propto C_1\left[DA_L+(DP_L-DP_L(c))+\tau DP_L(c)\right] \\
&+ \quad C_2\left[CA_L+(CP_L-CP_L(c))+\tau CP_L(c)\right]+\ldots && (30)
\end{aligned}
$$

Thus, if all the connected diagrams are about a factor of ξ smaller than the corresponding disconnected ones, it is very difficult to resurrect the $B_d^0\to\pi^0\pi^0$ amplitude, unless the matrix elements of the penguin operators Q_3–Q_{10} are very large. The same arguments, however, could be applied to kaon decays, with the surprising conclusion that $|A_0|\sim 2|A_2|$ in sharp disagreement with the experimental observation $|A_0|\gg|A_2|$. It is then clear that dynamical effects play a fundamental role in this game.

Of course, it is possible to argue that the dynamics of the decay for kaons and B-mesons is completely different and that factorization is a very bad approximation for light mesons. It is clear, however, that one cannot exclude some residual dynamical

[7] This could alternatively mean that factorization is a poor approximation.

effect which enhances the $B_d^0 \to \pi^0\pi^0$ amplitude over its factorized value. The contribution of Q_1 and Q_2 to A_0^t, non-zero phases δ_ξ and δ_L or the connected-disconnected diagram-exchange mechanism for CA_L and $CP_L - CP_L(c)$ discussed above may provide such effects.

5 Numerical results

In this section, we present numerical results for the quantities $\sin 2\alpha$ and R, that only depend on ratios of amplitudes. The latter are all proportional, via the parameters ξ, ..., η_6, to DE_L, the value of which cancels out in the ratios.

One could, however, also be interested to know the variation of $BR(B_d^0 \to \pi^+\pi^-)$ for different assumptions about GIM-penguin, charming-penguin, annihilation diagrams etc. Thus we also give below $R_{+-} = BR(B_d^0 \to \pi^+\pi^-)/BR(B_d^0 \to \pi^+\pi^-)|_{DE_L}$, where $BR(B_d^0 \to \pi^+\pi^-)$ is the branching ratio computed for a given set of the parameters ξ, ..., η_6, whilst $BR(B_d^0 \to \pi^+\pi^-)|_{DE_L}$ is the branching ratio with all the diagrams put to zero, but DE_L. In this way, the reader can use his preferred model to compute DE_L and predict the physical value of $BR(B_d^0 \to \pi^+\pi^-)$. In the following, R will also denote $BR(B_d^0 \to \pi^0\pi^0)/BR(B_d^0 \to \pi^+\pi^-)|_{DE_L}$.

For the determination of α and the relative error, we define

$$\sin 2\alpha^{eff} = \frac{Im\lambda}{|\lambda|}\,, \tag{31}$$

which is the quantity that can be extracted from the time-dependent asymmetry by measuring the coefficients of $\cos(\Delta M_d t)$ and of $\sin(\Delta M_d t)$ in eq. (1). The uncertainty on the "true" value of $\sin 2\alpha$ can be estimated by constructing

$$\Delta = \sin 2\alpha^{eff} - \sin 2\alpha\,. \tag{32}$$

Finally we present our results for the ratios $R_1 = BR(B_d^0 \to K^0\bar{K}^0)/BR(B_d^0 \to \pi^+\pi^-)|_{DE_L}$, $R_2 = BR(B^+ \to \pi^+K^0)/BR(B_d^0 \to \pi^+\pi^-)|_{DE_L}$ and $R_3 = BR(B_d^0 \to K^+\pi^-)/BR(B_d^0 \to \pi^+\pi^-)|_{DE_L}$, the values of which have a strong dependence on the contribution of charming-penguin diagrams.

In subsec. 5.1 the results for R and R_{+-} under different assumptions on the operator matrix elements are presented; in subsec. 5.2 the effects of these assumptions on the determination of $\sin 2\alpha$ are analyzed, while subsec. 5.3 contains the numerical results for R_1, R_2 and R_3.

5.1 Estimates of R and R_{+-}

Given the large number of parameters, in order to understand which diagrams give important/unimportant contributions, for several values of ξ and δ_ξ we vary one single of the η_is (and δ_L) of the set defined in sec. 4 at the time, while keeping all the others fixed to zero. We have also checked that the main features of the results discussed below are the same irrespectively of the choice of the RP and of the renormalization scale μ (2 GeV $\leq \mu \leq$ 10 GeV).

	C_1/C_2			
μ (GeV)	LO	NDR	HV	RI-Landau Gauge
2.0	-0.31	-0.27	-0.32	-0.24
5.0	-0.19	-0.16	-0.19	-0.15
10.0	-0.12	-0.09	-0.12	-0.08
	ξ			
μ (GeV)	LO	NDR	HV	RI-Landau Gauge
2.0	0.52(7)	0.49(8)	0.53(7)	0.46(8)
5.0	0.42(8)	0.39(9)	0.42(9)	0.39(9)
10.0	0.36(9)	0.33(9)	0.36(9)	0.32(9)

Table 1: *Values of C_1/C_2 and ξ for different RP and at different values of the renormalization scale μ. The values of ξ have been computed assuming $a_2/a_1 = 0.25 \pm 0.05$, from $B \to D\pi$, $D\rho$, $D^*\pi$ and $D^*\rho$ decays, and using $\xi = (a_2/a_1 - C_1/C_2)/(1 - a_2/a_1 \times C_1/C_2)$.*

a) Colour suppression for DE_L and CE_L Colour suppression depends on the value of the Wilson coefficients, ξ and the phase δ_ξ. Information on the value of ξ is usually obtained by analyzing several B-decay channels ($B \to D\pi$, $D\rho$, $D^*\pi$ and $D^*\rho$ [23]) and is correlated to the Wilson coefficients used in the analysis. In most of the cases, the leading order (LO) coefficients at $\mu = m_b$ are used and a value of $\xi \sim 0.4$ is found. From a comparison of the LO results, with those obtained at the next-to-leading order (NLO) in different renormalization schemes (NDR, HV and RI [22]), we find that the value of ξ is not very sensitive to the (considered) RP, whereas it can vary from 0.23, at $\mu = 10$ GeV, to 0.60, at $\mu = 2$ GeV [8]. The correlation between the ratio C_1/C_2 and the extracted value of ξ is shown in table 1. We have taken $a_2/a_1 = 0.25 \pm 0.05$, in agreement with most of the analyses of the experimental data [23]. In absence of a fully consistent treatment of the amplitudes at the NLO, which could be obtained if some lattice calculation existed [22], we have no reason to prefer a particular value of the scale, or to maintain any correlation between μ and the value of ξ. For this reason, in the following we take the coefficients computed at the LO for $\mu = 5$ GeV from ref. [22] but vary ξ in the range $0.2 \leq \xi \leq 0.5$, which covers almost all the values in table 1.

We have a comment on the choice of the Wilson coefficients made in some recent studies which may be useful to the reader. In refs. [5, 31] and [32] they used the renormalization scheme independent coefficients introduced in ref. [19], and computed for the full basis (3) in ref. [31]. Though perfectly legitimate, this choice corresponds to a value of the ratio $C_1/C_2 = -0.27$ (and to $\xi \sim 0.47$), sensibly larger than those found at leading order or at the NLO in the NDR, HV or RI schemes at a renormalization scale $\mu \sim m_b$, see for example ref. [22] [9].

On the basis of the discussion of the previous section, see eq. (29), for $\delta_\xi = 0$,

[8] This determination of ξ is only indicative, since it is not known whether the same value of ξ should be used for $B \to D\pi$ and $B \to \pi\pi$ decays.

[9] Indeed the renormalization scheme of ref. [19] has never been completely specified, because the external states on which the renormalization conditions were imposed were not given explicitly in the paper.

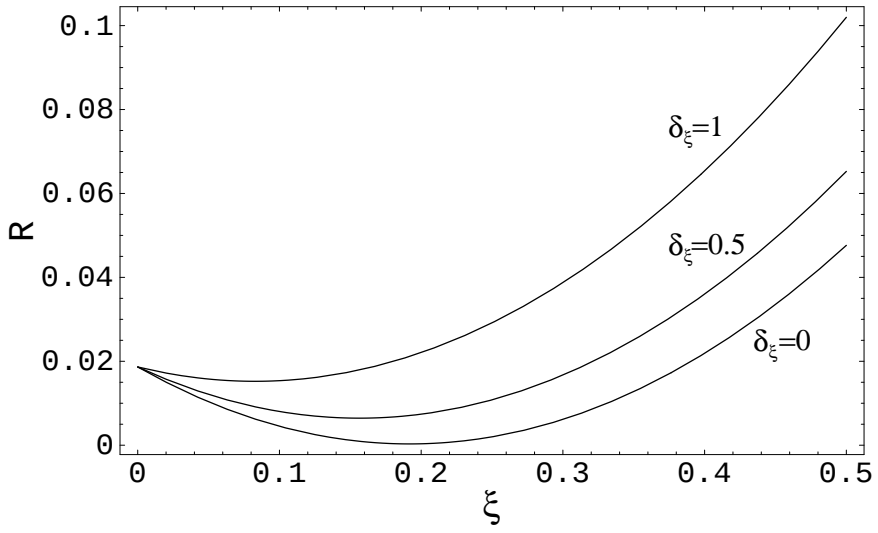

Figure 3: *The ratio R is given as a function of ξ at three values of δ_ξ. In the amplitudes, only contributions of emission diagrams are included.*

the ratio R has a minimum for $\xi \sim -C_1/C_2 \sim 0.2$ and rises for larger values of ξ. The suppression is softened for non-vanishing values of δ_ξ, as can be seen in fig. 3, and a value of $R = 0.03$–0.06 is obtained for $\xi \sim 0.4$–0.5 and $\delta_\xi = 0.5$ (to be compared to $R = 0.02$ at $\xi = 0$). Notice that R_{+-} only varies by less than 20 % in the range of ξ and δ_ξ considered here (it would only vary by about 10 %, as a function of δ_ξ, at $\xi = 0.4$ fixed).

b) Annihilation and GIM-penguin diagrams The effect of annihilation diagrams depends on δ_ξ and ξ. Let us first fix $\xi = 0.4$ and vary δ_ξ. For small values of δ_ξ, up to $\delta_\xi \sim 0.4$, R increases with η_A and reaches a value of ~ 0.1 at $\eta_A = 0.5$; for larger values of δ_ξ, instead, there is destructive interference which balances the positive effect of δ_ξ on colour suppression. The situation is illustrated in fig. 4. Contrary to R which is subject to appreciable variations, with the same parameters R_{+-} changes by less 20 % even at the largest value of η_A. Similar behaviours, but on different ranges of δ_ξ are observed at other values of ξ.

The effect of GIM-penguin diagrams is essentially the same as for annihilation diagrams, since, as can be immediately seen from eq. (26), the largest Wilson coefficient C_2 multiplies the combination $\eta_A + \eta_P$.

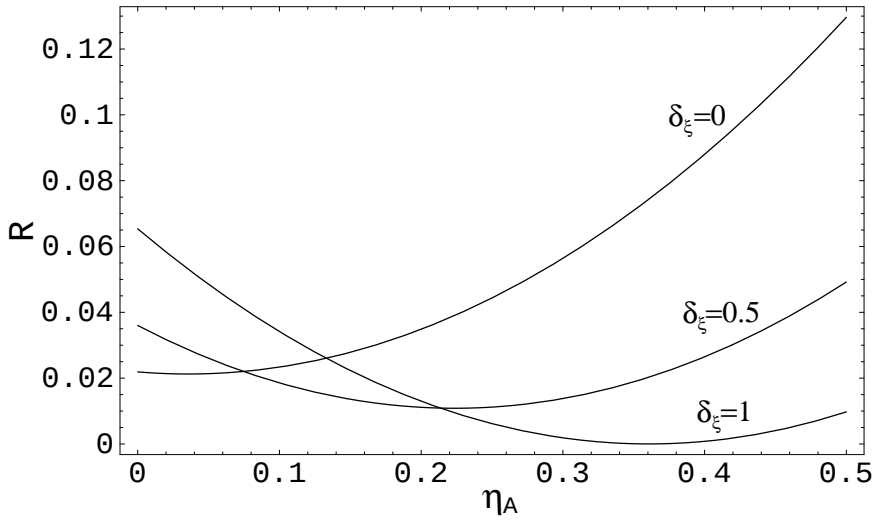

Figure 4: *The ratio R is given as a function of η_A at three values of δ_ξ. In the amplitudes, only contributions of annihilation and emission diagrams are included.*

c) Q_5 and Q_6 and Electro-penguins Q_5 and Q_6 give relatively small corrections both to R and R_{+-}, because their coefficients are very small. Of the two terms, the contribution of Q_5, which has the smaller coefficient and is colour suppressed, is always very small. Q_6 has the effect of changing by about $\sim 80\%$ and $\sim 5\%$ the ratios R and R_{+-} respectively when $\eta_6 = 2$. A large effect from Q_6 can only be obtained at extremely large values of its matrix element. In comparison, electro-penguin diagrams always give tiny corrections.

d) Charming penguins The most important of all the effects is given by charming penguins. The explanation was already given in the previous section: these diagrams correspond to the insertion of the operators Q_1 and Q_2 which have large Wilson coefficients and the contribution of which is also augmented by the factor τ. They may easily enhance the $B_d^0 \to \pi^0\pi^0$ amplitude, and change also appreciably the $B_d^0 \to \pi^+\pi^-$ rate.

In figs. 5 and 6, we give R and R_{+-} as a function of η_L at three value of δ_L (for $\xi = 0.4$ and $\delta_\xi = 0$). We observe that, for $\eta_L \sim 1.0$, there is a quite substantial effect when δ_L is different from zero: R can reach values as large

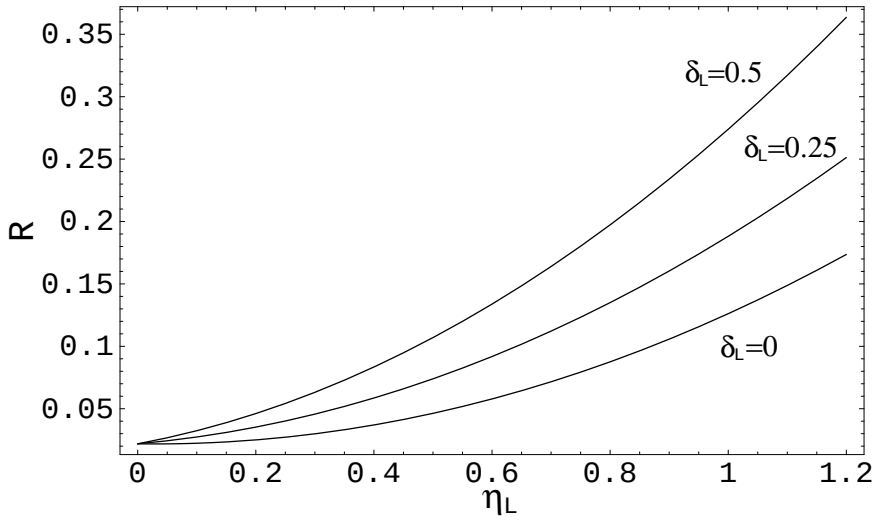

Figure 5: *The ratio R is given as a function of η_L at for $\delta_L = 0$, 0.25 and 0.50, at $\xi = 0.4$ and $\delta_\xi = 0$. In the amplitudes, only contributions of emission diagrams and charming penguins are included.*

as 0.25 (for $\delta_L = 0.25$) and even 0.35 for $\delta_L = 0.5$ [10]. Even with $\delta_L = 0$ we find a large enhancement, which can lead to $R = 0.10$–0.15 at relatively modest values of η_L. In this case there is even an increase of about 20% of R_{+-}. This discussion shows that values of $BR(B_d^0 \to \pi^0\pi^0)$ as large as $1\text{–}3 \times 10^{-6}$ (assuming $BR(B_d^0 \to \pi^+\pi^-) = 1\text{–}2 \times 10^{-5}$) are indeed easily possible.

5.2 Determination of $\sin 2\alpha$

In this subsection, we discuss the uncertainties in the determination of $\sin 2\alpha$. These uncertainties are parametrized in terms of the shift Δ introduced before. Δ is computed at different values of $\sin 2\alpha$ which are obtained by varying the CKM weak phase δ. The values of of $\sin 2\alpha$ are computed from the expression $\sin 2\alpha = Im(\tau/\tau^\star)$, with τ given in the last of eqs. (13), and using $\rho = \sigma \cos\delta$ and $\eta = \sigma \sin\delta$ with $\sigma = 0.36$ and $-0.8 \leq \cos\delta \leq +0.7$ ($\sin\delta \geq 0$). In the figures below, we give Δ as a function of

[10] The effect is striking for the $B_d^0 \to \pi^+\pi^-$ rate which at $\eta_L = 1.2$ and $\delta_L \sim 1.0$ almost vanishes. We believe, however, that this is a quite remote possibility.

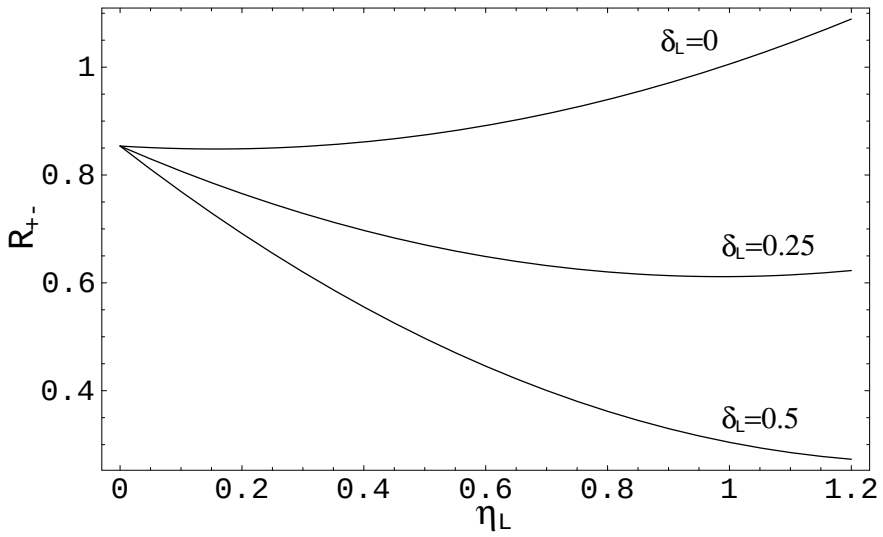

Figure 6: *The ratio R_{+-} is given as a function of η_L for $\delta_L = 0$, 0.25 and 0.50, at $\xi = 0.4$ and $\delta_\xi = 0$. In the amplitudes, only contributions of emission diagrams and charming penguins are included.*

$\sin 2\alpha^{eff}$ because the latter is the quantity which is measured experimentally. The strange behaviour of Δ for $\sin 2\alpha^{eff} \gtrsim 0.80$ comes from the fact that two different values of $\cos\delta$, for $\cos\delta \lesssim -0.6$, correspond to the same value of $\sin 2\alpha$. Had we varied $\cos\delta$ within the range allowed by the combined analysis of the K^0–$\bar{K}^0$ and of the B_d^0–$\bar{B}_d^0$ mixing amplitudes [33], i.e. $-0.3 \leq \cos\delta \leq 0.9$, the two-fold ambiguity would have disappeared, because the interval in $\cos\delta$ limits, in this case, $\sin 2\alpha$ to values smaller than about 0.9.

In the following, we discuss together the cases a)–c) of subsec. 5.1 and the case d) separately.

a)–c) In fig. 7 we show a band of possible values for Δ. This band has been obtained in the following way: a) by varying ξ between 0.0 and 0.5 with $\delta_\xi = 0$, 0.5 and 1.0, and all the other η_i's taken to be zero; b) by fixing $\xi = 0.4$ and varying η_A between 0.0 and 0.5 with $\delta_\xi = 0$, 0.5 and 1.0 ($\eta_P = \eta_5 = \eta_6 = \eta_L = 0$); c) by taking $\xi = 0.4$, $\delta_\xi = 0$ and $0.0 \leq \eta_6 \leq 2.0$ ($\eta_A = \eta_P = \eta_5 = \eta_L = 0$). We see that for all the cases a)-c) the size of Δ is about $-(0.05$–$0.15)$ in almost the

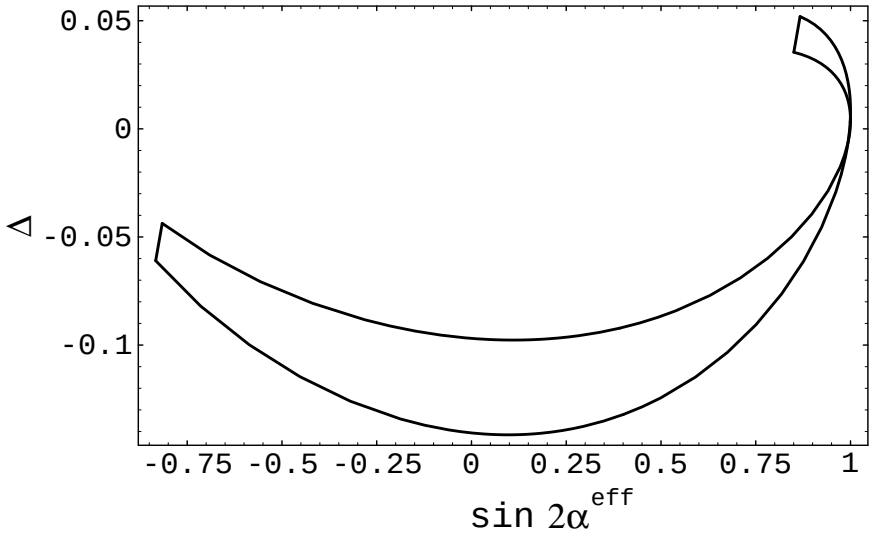

Figure 7: *A band of possible values for* Δ *as a function of* $\sin 2\alpha$ *is given. This band corresponds to different choices of the parameters introduced in 1)–5), see sec. 4.*

whole interval of values of $\sin 2\alpha$ [11]. This happens because the terms depending on ξ, δ_ξ, η_A and $\eta_{5,6}$ give small variations (of the order of 20% at most) to the $B_d^0 \to \pi^+\pi^-$ amplitude. These results are similar to those found in refs. [5, 32] where different hypotheses or approximations where used.

d) We varied η_L and δ_L as at the point d) of subsection 5.1, while taking $\xi = 0.4$ and δ_ξ and all the other η_is to be zero. In this case the uncertainty on $\sin 2\alpha$ can be very large, corresponding to $\Delta \sim 0.4$–0.8, see fig. 8. The reason, as already discussed above, is that charming penguins give large corrections to the $B_d^0 \to \pi^+\pi^-$ amplitude too, while in the other cases considered above [a)–c)], the corrections are large only for the $B_d^0 \to \pi^0\pi^0$ amplitude where large cancellations occur.

In order to guide the reader, we end this subsection by giving in table 2 a set of numerical results for $\sin 2\alpha^{eff}$ and Δ obtained for different choices of the parameters introduced in a)–d) (also reported in the table). In the set of examples given in table 2, $\Delta \lesssim 0.6$.

[11] Smaller values are only found when $\sin 2\alpha$ is close to $+1$ or -1.

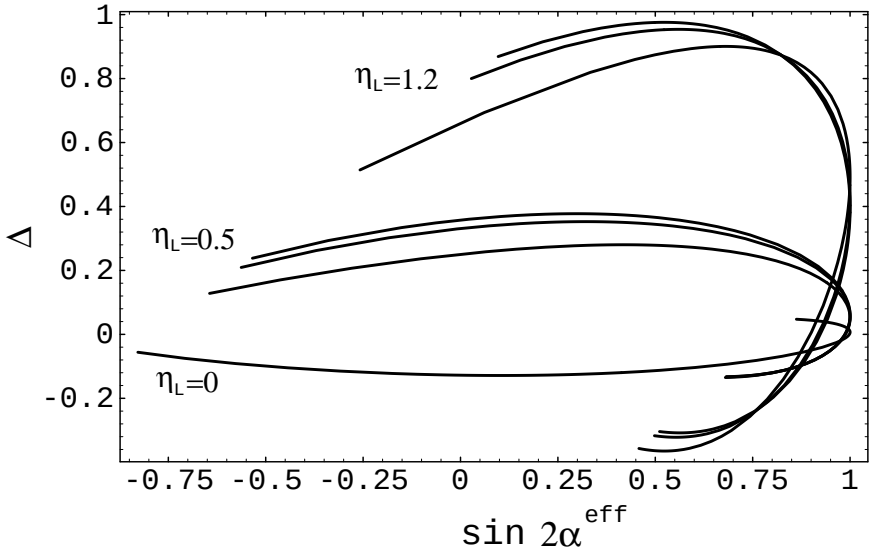

Figure 8: *A family of curves for* Δ *is given as a function of* $\sin 2\alpha$*. They correspond to different choices of the parameters* η_L *(*$\eta_L = 0,\ 0.5,\ 1.2$*) and* δ_L *(*$\delta_L = 0,\ 0.25,\ 0.5$*) introduced in d), see sec. 4.*

5.3 Charming-penguin dominated branching ratios

Our main results for the ratios of rates introduced before are summarized in table 3, where a large set of possibilities has been considered. We have introduced a label "No." to distinguish the different cases which will be discussed below [12]. The table is instructive because it shows the strong correlation between R and $R_{1,2,3}$, particularly when charming-penguin contributions are large. We will make use of this correlation, combined to the experimental information $BR(B_d^0 \to K^+\pi^-) = (1.5^{+0.5}_{-0.4} \pm 0.2) \times 10^{-5}$ and $BR(B_d^0 \to \pi^+\pi^-) < 1.5 \times 10^{-5}$ [9], and to prejudices based on theoretical estimates of the matrix elements, in order to reduce the uncertainties. Given the present precision in the measurement of $BR(B_d^0 \to K^+\pi^-)$, and our ignorance on the matrix elements, the discussion below is, at the moment, preliminary and semi-quantitative and only intended to illustrate a method which may become very useful when the experimental precision will increase and theoretical predictions for GIM- and charming-penguin diagrams will become available.

[12] In order to check the stability of the results, other cases have been analyzed but not given in table 3.

No.	$\sin 2\alpha^{eff}$	Δ	$\sin 2\alpha^{eff}$	Δ
	$\cos\delta = -0.8$, $\sin 2\alpha = 0.81$		$\cos\delta = 0$, $\sin 2\alpha = 0.64$	
2	0.86	0.047	0.53	−0.11
7	0.68	−0.13	0.88	0.24
8	0.68	−0.13	0.88	0.23
9	0.68	−0.14	0.85	0.21
14	0.73	−0.087	0.8	0.16
15	0.62	−0.2	0.96	0.31
18	0.72	−0.09	0.82	0.17
23	0.61	−0.2	0.96	0.32
27	0.65	−0.17	0.92	0.28
	$\cos\delta = 0.38$, $\sin 2\alpha = -0.04$		$\cos\delta = 0.7$, $\sin 2\alpha = -0.77$	
2	−0.16	−0.12	−0.83	−0.056
7	0.34	0.38	−0.53	0.24
8	0.32	0.35	−0.56	0.21
9	0.24	0.27	−0.64	0.13
14	0.17	0.21	−0.67	0.11
15	0.53	0.57	−0.36	0.42
18	0.21	0.25	−0.63	0.14
23	0.52	0.56	−0.38	0.39
27	0.43	0.47	−0.47	0.3

Table 2: *We give results for* $\sin 2\alpha^{eff}$ *and* Δ *obtained with different choices of the parameters* δ_ξ, ..., $\eta_i s$. *In all cases* $\xi = 0.4$. *In the table, the value of* $\cos\delta$ *used in the different examples, and the corresponding value of* $\sin\alpha$, *are also shown. The label "No.", which is the same of table 3, allows a study of the correlation between* Δ *and the values of the branching ratios discussed in subsec. 5.3.*

We proceed as follows:

i) $\underline{BR(B_d^0 \to \pi^+\pi^-)}$ Different theoretical estimates of this branching ratio, obtained by using the factorization hypothesis but with different models to evaluate the matrix elements, are consistent within a factor of two and give $BR(B_d^0 \to \pi^+\pi^-) =$ 1–2 $\times 10^{-5}$ [3]–[5]. The spread of these predictions is mostly due to differences in the values of the form factors of the weak-currents and in the value of ξ used for the calculation of the emission diagrams. The results, instead, are only marginally affected by the contribution of the penguin operators Q_3–Q_{10}, which in some cases have been omitted (charming-penguin diagrams have never been considered). This happens for the following reason: in the factorized case the matrix elements of Q_5 and Q_6, which are expected to give the largest contributions of all penguin operators, correspond to $\eta_{5,6} \sim 1$ for which the correction is of a few percent, as can been seen by comparing No. 2 to No. 5 in table 3. This explains the relative stability of the theoretical results. We then assume that 1–2 $\times 10^{-5}$ is a range representative of the theoretical uncertainty for emission diagrams [13]. On the basis of the above discussion, in the following we consider

[13] Predictions on $BR(B_d^0 \to \pi^0\pi^0)$ are, instead, very unstable because in this case even a small error on

three possibilities $BR(B_d^0 \to \pi^+\pi^-)|_{DE+CE} = (0.5, 1.0, 1.5) \times 10^{-5}$. The latter two cases have been used because they are in the ballpark of all estimates, the first value because it accounts for large deviations from the factorization predictions. Values of $BR(B_d^0 \to \pi^+\pi^-)|_{DE+CE}$ larger than 2×10^{-5} are excluded on the basis of ii) below. $BR(B_d^0 \to \pi^+\pi^-)|_{DE+CE}$ corresponds to the case No. 2 of table 3, where $R_{+-} = 0.85$. Thus, for example, if we assume $BR(B_d^0 \to \pi^+\pi^-)|_{DE+CE} = 1.5 \times 10^{-5}$, the ratio $R = 0.54$ (No. 18) gives $BR(B_d^0 \to \pi^0\pi^0) = 0.54/0.85 \times 1.5 \times 10^{-5} = 0.95 \times 10^{-5}$.

ii) $\underline{BR(B_d^0 \to K^+\pi^-) \text{ vs } BR(B_d^0 \to \pi^+\pi^-)}$ From CLEO we expect $BR(B_d^0 \to K^+\pi^-)$ to be larger than $BR(B_d^0 \to \pi^+\pi^-)$. Thus we exclude all those cases where $BR(B_d^0 \to K^+\pi^-) \leq BR(B_d^0 \to \pi^+\pi^-)$, namely No. 1–6, 13, 17, 18, 21, 22, 25, 26.

iii) $\underline{BR(B_d^0 \to K^+\pi^-)}$ We also exclude all cases where $BR(B_d^0 \to K^+\pi^-) \leq 1 \times 10^{-5}$ or $BR(B_d^0 \to K^+\pi^-) \geq 2 \times 10^{-5}$.

Indeed, from the experimental results, $BR(B_d^0 \to K^+\pi^-) \sim 2.5 \times 10^{-5}$ or $BR(B_d^0 \to K^+\pi^-) \sim 0.5 \times 10^{-5}$ and also $BR(B_d^0 \to K^+\pi^-) \sim BR(B_d^0 \to \pi^+\pi^-)$ are still open possibilities. However, we want to stretch here the experimental constraints in order to show how this analysis works.

We now discuss the results of table 4, where the main results of the selection based on i)–iii) are given. For comparison, in this table we also give the results for No. 2, where only emission diagrams contribute. We first notice that the charming-penguin enhancement of $BR(B^+ \to \pi^+K^0)$ and $BR(B_d^0 \to K^+\pi^-)$ is always very large, corresponding to a factor of 10–40, with respect to standard case No. 2. A stable prediction of the results in the table is that we also expect $BR(B^+ \to \pi^+K^0)$ to be comparable to $BR(B_d^0 \to K^+\pi^-)$ and of the order 1×10^{-5}. Although, on the basis of table 3, a much large enhancement of $BR(B_d^0 \to \pi^0\pi^0)$ would be possible, the constraints i)–iii) limit the effect of charming penguins so that the final result is about a factor of 2 larger than previous estimates [3, 4]. A larger enhancement is still possible, however, if we relax the selection constraints. For example, without ii), case No. 18 is acceptable and, for $BR(B_d^0 \to \pi^+\pi^-)|_{DE+CE} = 0.5 \times 10^{-5}$, it gives

$$\begin{aligned} BR(B_d^0 \to \pi^+\pi^-) &= 1.2 \times 10^{-5}\,, \qquad BR(B_d^0 \to \pi^0\pi^0) = 0.3 \times 10^{-5}\,, \\ BR(B_d^0 \to K^0\bar{K}^0) &= 0.3 \times 10^{-5}\,, \qquad BR(B^+ \to \pi^+K^0) = 0.6 \times 10^{-5}\,, \\ BR(B_d^0 \to K^+\pi^-) &= 0.8 \times 10^{-5}\,. \end{aligned} \tag{33}$$

These results give a large $BR(B_d^0 \to \pi^0\pi^0)$, and are still compatible with the experimental measurement of $BR(B_d^0 \to K^+\pi^-)$ and the present limit on $BR(B_d^0 \to \pi^+\pi^-)$. This example also show the importance of the reduction of the experimental error for determining charming-penguin effects.

We finally notice that for $BR(B_d^0 \to K^0\bar{K}^0)$, besides charming penguins, GIM-penguins are also relatively important. Moreover GIM- and charming-penguin diagrams appear in the r.h.s. of eq. (15) in the same combination as in A_0^t, eq. (27). A

the evaluation of a single diagram is amplified by the large cancellations of the different contributions. This is also shown by comparing different entries in the table, where variations of R over one order of magnitude are observed.

measurement of $BR(B_d^0 \to K^0\bar{K}^0)$ is then very important for the determination of the combined value of GIM and charming-penguin diagrams in $B_d^0 \to \pi\pi$ decays and may lead to a reduction of the uncertainties in the determination of $\sin 2\alpha$. Unfortunately, in most of the cases, this branching ratio remains rather small, $BR(B_d^0 \to K^0\bar{K}^0) \sim 5 \times 10^{-7}$, in spite of the enhancement due to charming penguins. For this reason this may be a difficult measurement even for B-factories. However, from the example discussed in (33) and the results of the table, a $BR(B_d^0 \to K^0\bar{K}^0) = 2\text{–}3 \times 10^{-6}$ is still compatible with the present experimental constraints and the experimental search of this decay mode is very important.

6 Conclusions

In this paper we have discussed several effects which could enhance the $B_d^0 \to \pi^0\pi^0$ branching ratio. Among these, we have shown the presence of diagrams involving operators containing charmed quarks, denoted as "charming penguins", which were never studied before. Since there is no reason *a priori* to expect the value of these diagrams to be small, and the corresponding Wilson coefficients are of $O(1)$, and not of $O(\alpha_s/12\pi \ln(m_t^2/\mu^2))$, they may have a large effect in the $B_d^0 \to \pi^0\pi^0$ decay rate and in the determination of the weak phase α extracted from the measurement of the $B_d^0 \to \pi^+\pi^-$ time-dependent asymmetry. In absence of any realistic estimate of the value of charming-penguin diagrams, we allow them to vary within reasonable ranges of values and show that, without further constraints, they can lead to a $BR(B_d^0 \to \pi^0\pi^0) \sim 1\text{–}3 \times 10^{-6}$. Correspondingly, the uncertainty in determination of $\sin 2\alpha$ from the time-dependent asymmetry could be as large as 0.4–0.8.

We have also shown that GIM- and charming-penguin diagrams dominate the $B_d^0 \to K^0\bar{K}^0$ amplitude because emission and annihilation diagrams are only produced by the insertion of the operators Q_3–Q_{10} which have rather small Wilson coefficients. GIM- and charming-penguin diagrams appear in the $B_d^0 \to K^0\bar{K}^0$ amplitude in the same combination as in the $B_d^0 \to \pi\pi$ case. Thus, if we assume $SU(3)$ symmetry, a measurement of $BR(B_d^0 \to K^0\bar{K}^0)$ contains important information on these contributions and may help to reduce the uncertainty in the extraction of $\sin 2\alpha$ from the $B_d^0 \to \pi^+\pi^-$ time-dependent asymmetry.

A striking effect of charming-penguins occurs in $B^+ \to \pi^+K^0$ and $B_d^0 \to K^+\pi^-$ decays. In this case, the enhancement easily gives values of $BR(B^+ \to \pi^+K^0)$ and $BR(B_d^0 \to K^+\pi^-)$ of about 1×10^{-5}, 10–40 times larger than those obtained by considering emission diagrams only. This is because in the latter case the main contribution is Cabibbo suppressed. Our findings are supported by the recent results of the CLEO Collaboration [9]. Theoretical predictions of the charming-penguin (and GIM-penguin) amplitudes, either from the lattice, or with QCD sum rules, or with any other non-perturbative technique, are then urgently needed.

Acknowlegments

We thank F. Ferroni, M. Giorgi, M. Gronau, A. Masiero, O. Pène, R. Poling and A. Pugliese for very useful discussions. We acknowledge the partial support by the

EC contract CHRX-CT93-0132. G.M. acknowledges the Phys. Dept. of the Universidad Autónoma de Madrid for its hospitality and the Fundacion IBERDROLA for its support. We acknowledge partial support by M.U.R.S.T.

References

[1] I.I. Bigi and A.I. Sanda, Nucl. Phys. B281 (1987) 41; Y. Nir and H.R. Quinn, Ann. Rev. Nucl. Part. Sci. 42 (1992) 211.

[2] M. Gronau and D. London, Phys. Rev. Lett. 65 (1990) 3381.

[3] Deandrea et al., Phys. Lett. B318 (1993) 549.

[4] G. Kramer and W.F. Palmer, Phys. Rev. D52 (1995) 6411.

[5] R. Aleksan et al., Phys. Lett. B356 (1995) 95.

[6] M. Bauer, B. Stech and M. Wirbel, Z. Phys. C29 (1985) 637; C34 (1987) 103; N. Isgur, D. Scora, B. Grinstein and M.B. Wise, Phys. Rev. D39 (1989) 799; N. Isgur and D. Scora, Phys. Rev. D40 (1989) 1491; F.J. Gilman and R.R. Singleton, Phys. Rev. D41 (1990) 142.

[7] V.M. Belayev et al. Phys. Rev. D51 (1995) 6177; P. Ball, Phys. Rev. D48 (1993) 3190; P. Ball and V.M. Braun, Phys. Rev. D54 (1996) 2182.

[8] ELC Collaboration, A. Abada et al., Nucl. Phys. B416 (1994) 675; APE Collaboration, C.R. Allton et al., Phys. Lett. B345 (1995) 513; UKQCD Collaboration, D.R. Burford et al., Nucl. Phys. B447 (1995) 425; UKQCD Collaboration, J.M. Flynn et al., Nucl. Phys. B461 (1996) 327.

[9] The CLEO Collaboration, presented by J. Fast at "Les Rencontres de Physique de la Vallée de Aoste", La Thuile, March 5th 1997, to appear in the Proceedings.

[10] M. Ciuchini, E. Franco, G. Martinelli and L. Silvestrini, in preparation.

[11] M.A. Shifman , A.I. Vainshtein and V.I. Zakharov, Nucl. Phys. B120 (1977) 316; JEPT (Sov. Phys.) 45 (1977) 670.

[12] F.J. Gilman and M. Wise, Phys. Rev. D27 (1983) 1128.

[13] J. Bijnens and M. Wise, Phys. Lett. B137 (1984) 245.

[14] M. Lusignoli, Nucl. Phys. B325 (1989) 33.

[15] M. Gronau, O.F. Hernandéz, D. London and J.L. Rosner, Phys. Rev. D50 (1994) 4529; D52 (1995) 6374; Phys. Lett. B333 (1994) 500; M. Gronau, D. London and J.L. Rosner, Phys. Rev. Lett. 73 (1994) 21.

[16] L. Wolfenstein, Phys. Rev. Lett. 51 (1983) 1945.

[17] G. Altarelli, G. Curci, G. Martinelli and S. Petrarca Nucl. Phys. B187 (1981) 461.

[18] A.J. Buras, P.H. Weisz, Nucl. Phys. B333 (1990) 66.

[19] A.J. Buras, M. Jamin, M.E. Lautenbacher and P.H. Weisz, Nucl. Phys. B370 (1992) 69, Addendum, ibid. Nucl. Phys. B375 (1992) 501.

[20] A.J. Buras, M. Jamin and M.E. Lautenbacher, Nucl. Phys. B400 (1993) 37 and B400 (1993) 75.

[21] M. Ciuchini, E. Franco, G. Martinelli and L. Reina, Nucl. Phys. B415 (1994) 403.

[22] M. Ciuchini, E. Franco, G. Martinelli, L. Reina and L. Silvestrini, Z. Phys. C68 (1995) 239.

[23] H. Yamamoto, HUTP-94-A006, hep-ph/9403255; H.-Y. Cheng and B. Tseng, Phys. Rev. D51 (1995) 6259; T.-W. Yeh, H. Li, CCUTH-96-07, hep-ph/9701233v2 and refs. therein.

[24] J.F. Donoghue, E. Golowich, A.A. Petrov and J.M. Soares, Phys. Rev. Lett. 77 (1996) 2178.

[25] G. Nardulli and T.N. Pham, Phys. Lett. B391 (1997) 165.

[26] F. Buccella et al., Phys. Rev. D51 (1995) 3478; F. Buccella, M. Lusignoli and A. Pugliese, Phys. Lett. B379 (1996) 249.

[27] P. Zenczykowski, INP-1712-PH, hep-ph/9601265.

[28] B. Blok, M. Gronau and J.L. Rosner, EFI-97-04, hep-ph/9701396.

[29] J. Flynn, rapporteur talk given at Latt96, 14th International Symposium on Lattice Field Theory, St. Louis, 4-8 June 1996, to appear in the Proceedings, hep-lat/9610010; G. Martinelli, Nucl. Instrum. Meth. A384 (96) 241 and refs. therein.

[30] M.B. Gavela et al., Phys. Lett. 211B (1988) 139; C. Bernard and A. Soni, Nucl. Phys. B (Proc. Suppl.) 17 (1990) 495 and refs. therein.

[31] N.G. Deshpande and X.-G. He, Phys. Rev. Lett. 74 (1995) 26.

[32] P.S. Marrocchesi and N. Paver, hep-ph/9702353.

[33] M. Ciuchini, CERN-TH/97-2, hep-ph/9701278, to appear in the Proceedings of the 4th KEK Topical Conference on "Flavor Physics", KEK, Japan, 29-31 October 1996; see also ref. [22].

No.	ξ	δ_ξ	$\eta_{A,P}$	$\eta_{5,6}$	η_L	δ_L	$\mathcal{R}$	$\mathcal{R}_{+-}$	$\mathcal{R}_1$	$\mathcal{R}_2$	$\mathcal{R}_3$
1	0	0	0	0	0	0	0.019	1.	0.0044	0.11	0.083
2	0.4	0	0	0	0	0	0.022	0.85	0.0025	0.061	0.076
3	0.4	0.5	0	0	0	0	0.036	0.87	0.0028	0.067	0.075
4	0.4	0	0.25	0	0	0	0.13	1.1	0.04	0.083	0.13
5	0.4	0	0	1	0	0	0.025	0.87	0.013	0.31	0.3
6	0.4	0	0	2	0	0	0.032	0.89	0.031	0.75	0.71
7	0.4	0	0	0	0.5	0	0.046	0.87	0.034	0.82	0.94
8	0.4	0	0	0	0.5	0.25	0.074	0.67	0.042	1.	1.3
9	0.4	0	0	0	0.5	0.5	0.11	0.5	0.066	1.6	2.1
10	0.4	0	0	0	1	0	0.13	1.	0.18	4.3	4.5
11	0.4	0	0	0	1	0.25	0.19	0.61	0.21	5.	5.6
12	0.4	0	0	0	1	0.5	0.27	0.3	0.29	7.1	8.1
13	0.4	0.5	0	1	0.5	0	0.016	0.86	0.014	0.34	0.46
14	0.4	0.5	0	1	0.5	0.25	0.043	0.66	0.027	0.65	0.93
15	0.4	0.5	0	2	1	0	0.025	0.9	0.084	2.	2.3
16	0.4	0.5	0	2	1	0.25	0.089	0.52	0.13	3.1	3.7
17	0.4	0.5	0.25	0	0.5	0	0.15	1.3	0.19	0.74	0.89
18	0.4	0.5	0.5	0	0.5	0.25	0.54	2.	0.45	0.98	1.4
19	0.4	0.5	0.25	0	1	0	0.3	1.7	0.45	4.	4.3
20	0.4	0.5	0.5	0	1	0.25	0.82	2.3	0.82	4.8	5.6
21	0.4	0.5	0.25	1	0.5	0	0.12	1.2	0.14	0.3	0.43
22	0.4	0.5	0.5	1	0.5	0.25	0.47	1.8	0.37	0.63	1.1
23	0.4	0.5	0.25	1	1	0	0.25	1.5	0.36	2.9	3.1
24	0.4	0.5	0.5	1	1	0.25	0.74	2.2	0.71	3.8	4.6
25	0.4	0.5	0.25	2	0.5	0	0.09	1.1	0.093	0.061	0.17
26	0.4	0.5	0.5	2	0.5	0.25	0.42	1.7	0.3	0.48	0.9
27	0.4	0.5	0.25	2	1	0	0.21	1.4	0.29	1.9	2.1
28	0.4	0.5	0.5	2	1	0.25	0.67	2.	0.61	3.	3.8

Table 3: *We give results for* $R = BR(B_d^0 \to \pi^0\pi^0)/BR(B_d^0 \to \pi^+\pi^-)|_{DE_L}$, $R_{+-} = BR(B_d^0 \to \pi^+\pi^-)/BR(B_d^0 \to \pi^+\pi^-)|_{DE_L}$, $R_1 = BR(B_d^0 \to K^0\bar{K}^0)/BR(B_d^0 \to \pi^+\pi^-)|_{DE_L}$, $R_2 = BR(B^+ \to \pi^+K^0)/BR(B_d^0 \to \pi^+\pi^-)|_{DE_L}$ *and* $R_3 = BR(B_d^0 \to K^+\pi^-)/BR(B_d^0 \to \pi^+\pi^-)|_{DE_L}$, *obtained with different choices of the parameters* ξ, ..., $\eta_i s$.

No.	$B_d^0 \to \pi^+\pi^-$ $BR \times 10^5$	$B_d^0 \to \pi^0\pi^0$ $BR \times 10^5$	$B_d^0 \to K^0\bar{K}^0$ $BR \times 10^5$	$B^+ \to \pi^+K^0$ $BR \times 10^5$	$B_d^0 \to K^+\pi^-$ $BR \times 10^5$
$BR(B_d^0 \to \pi^+\pi^-)_{DE+CE} = 1.5 \times 10^{-5}$					
2	1.5	0.05	0.004	0.11	0.13
7	1.5	0.08	0.06	1.4	1.7
14	1.2	0.08	0.05	1.1	1.6
$BR(B_d^0 \to \pi^+\pi^-)_{DE+CE} = 1 \times 10^{-5}$					
2	1	0.03	0.003	0.07	0.09
7	1	0.05	0.04	1	1.1
8	0.8	0.09	0.05	1.2	1.5
14	0.8	0.05	0.03	0.8	1.1
$BR(B_d^0 \to \pi^+\pi^-)_{DE+CE} = 0.5 \times 10^{-5}$					
2	0.5	0.01	0.001	0.04	0.04
9	0.3	0.06	0.04	0.9	1.2
15	0.5	0.01	0.05	1.2	1.4
23	0.9	0.1	0.2	1.7	1.8
27	0.8	0.1	0.2	1.1	1.2

Table 4: *Branching ratios for* $B_d^0 \to \pi^+\pi^-$, $B_d^0 \to \pi^0\pi^0$, $B_d^0 \to K^0\bar{K}^0$, $B^+ \to \pi^+K^0$ *and* $B_d^0 \to K^+\pi^-$. *The cases are labeled as in table 3. The BRs are normalized assuming three different values of* $BR(B_d^0 \to \pi^+\pi^-)|_{DE+CE}$.